HHS Public Access

Author manuscript

*Cancer Cell*. Author manuscript; available in PMC 2016 December 14.

Published in final edited form as:

*Cancer Cell*. 2015 December 14; 28(6): 773–784. doi:10.1016/j.ccell.2015.11.006.

# Extreme vulnerability of *IDH1* mutant cancers to NAD+ depletion

**Kensuke Tateishi**[1,9,10], **Hiroaki Wakimoto**[1,9,10], **A. John Iafrate**[3,9,10], **Shota Tanaka**[2,9,10], **Franziska Loebel**[1,9,10], **Nina Lelic**[1,9,10], **Dmitri Wiederschain**[5], **Olivier Bedel**[5], **Gejing Deng**[5], **Bailin Zhang**[5], **Timothy He**[5], **Xu Shi**[6,10], **Robert E. Gerszten**[6,10], **Yiyun Zhang**[6,10], **Jing-Ruey J. Yeh**[6,10], **William T. Curry**[1,10], **Dan Zhao**[2,9,10], **Sudhandra Sundaram**[2,9,10], **Fares Nigim**[1,9,10], **Mara V. A. Koerner**[1,9,10], **Quan Ho**[3,10], **David E. Fisher**[7,10], **Elisabeth M. Roider**[7,10], **Lajos V. Kemeny**[7,10], **Yardena Samuels**[8], **Keith T. Flaherty**[4,10], **Tracy T. Batchelor**[2,9,10], **Andrew S. Chi**[2,9,10,*], and **Daniel P. Cahill**[1,9,10,*]

[1]Department of Neurosurgery

[2]Divisions of Neuro-Oncology and Hematology/Oncology, Department of Neurology

[3]Department of Pathology

[4]Division of Hematology/Oncology

[5]Sanofi Oncology, Cambridge, Massachusetts, 02139, USA

[6]Cardiovascular Research Center, Cardiology Division, Department of Medicine

[7]Department of Dermatology

[8]Weizmann Institute of Science, Rehovot, Israel

[9]Translational Neuro-Oncology Laboratory

[10]Massachusetts General Hospital, Harvard Medical School, Boston, MA, 02114, USA

## Summary

Heterozygous mutation of *IDH1* in cancers modifies IDH1 enzymatic activity, reprogramming metabolite flux and markedly elevating 2-hydroxyglutarate (2-HG). Here, we found that 2-HG depletion did not inhibit growth of several *IDH1* mutant solid cancer types. To identify other metabolic therapeutic targets, we systematically profiled metabolites in endogenous *IDH1* mutant

[*]Corresponding Authors: Andrew S. Chi (current address: NYU Langone Medical Center, Laura and Isaac Perlmutter Cancer Center, 240 E. 38th St. 19th Floor, New York, NY 10016, chia01@nyumc.org; Daniel P. Cahill, cahill@mgh.harvard.edu.

**Accession Number**

The genome-wide DNA methylation data have been submitted to the GEO public database at http://www.ncbi.nlm.nih.gov/geo/ (accession number GSE73270).

**AUTHOR CONTRIBUTIONS**

K.T. and H.W. designed and performed experiments, interpreted data and wrote the paper. H.W., S.T., K.T., A.C. and W.C. generated cell lines. N.L., M.K. and S.S. sequenced samples. D.W., O.B., G.D., B.Z. and T.H. synthesized and characterized IDHi and performed measurements of 2-HG and IDHi. X.S., R.G., Y.Z. and J.-R.Y profiled metabolites. F.L., D.Z., F.N., Q.H., E.R. and L.K performed experiments. A.I., K.F. D.E.F., Y.S. and T.B. designed experiments and interpreted data. A.C and D.C. conceptualized the study, designed experiments, interpreted data and wrote the paper.

cancer cells after mutant IDH1 inhibition and discovered a profound vulnerability to depletion of the coenzyme NAD+. Mutant *IDH1* lowered NAD+ levels by downregulating the NAD+ salvage pathway enzyme nicotinate phosphoribosyltransferase (Naprt1), sensitizing to NAD+ depletion via concomitant nicotinamide phosphoribosyltransferase (NAMPT) inhibition. NAD+ depletion activated the intracellular energy sensor AMPK, triggered autophagy and resulted in cytotoxicity. Thus, we identify NAD+ depletion as a metabolic susceptibility of *IDH1* mutant cancers.

## Graphical Abstract

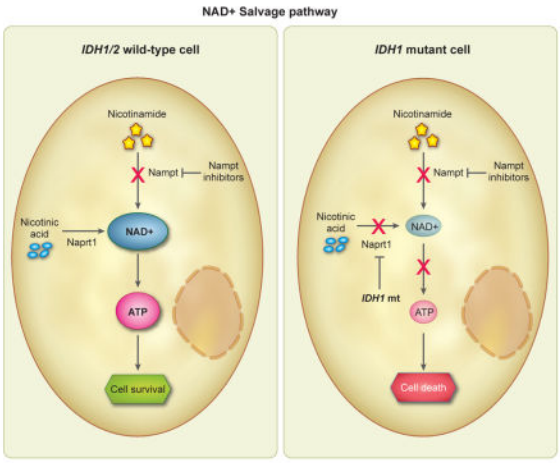


## INTRODUCTION

Accumulating evidence indicates that mutations in canonical metabolic enzymes can promote the development of cancer. Germline mutations in the tricarboxylic acid (TCA) cycle enzyme succinate dehydrogenase (*SDH*) give rise to familial paraganglioma and pheochromocytoma, and germline fumarate hydratase (*FH*) mutations result in familial forms of renal cell cancer (Kaelin, 2009). More recently, recurrent somatic mutations in the isocitrate dehydrogenase 1 (*IDH1*) and *IDH2* genes have been identified in a large fraction of gliomas, acute myeloid leukemias (AML), angioimmunoblastic T-cell lymphomas (AITL), chondrosarcomas and cholangiocarcinomas.

In gliomas, approximately 90% of *IDH1/2* mutations are arginine to histidine heterozygous substitutions in codon 132 of the *IDH1* gene (R132H). A small fraction of the *IDH1/2* mutations found in gliomas are different amino acid substitutions at the R132 position of *IDH1* or substitutions of the structurally analogous R172 residue of the homolog *IDH2* (Balss et al., 2008; Hartmann et al., 2009; Parsons et al., 2008; Yan et al., 2009). In contrast, the most common mutation in cartilaginous tumors is *IDH1* R132C (40%) (Amary et al., 2011; Kipp et al., 2012; Wang et al., 2013a), whereas in AML and AITL, *IDH2* mutations are most common (Marcucci et al., 2010; Mardis et al., 2009; Ward et al., 2012; Cairns et al., 2012). Essentially all of the mutations in *IDH1/2* result in heterozygous amino acid substitutions within a few targeted hotspot loci, suggesting an oncogenic functional contribution of mutant *IDH1/2* to tumorigenesis (Vogelstein et al., 2013). A shared consequence of these *IDH1/2* mutations is the near-complete elimination of the normal

oxidation and decarboxylation of isocitrate to alpha-ketoglutarate (a-KG) (Zhao et al., 2009; Yan et al., 2009) and the neomorphic overproduction of 2-hydroxyglutarate (2-HG) via NADPH-mediated reduction of a-KG (Dang et al., 2009). 2-HG is a byproduct metabolite that is otherwise produced at only modest levels in hypoxic states (Wise et al., 2011).

2-HG has therefore been proposed as an "oncometabolite" mediator of tumorigenesis in mutant *IDH1/2* cancers. 2-HG has been shown to inhibit a range of a-KG-dependent dioxygenases, including hypoxia inducible factor (HIF) hydroxylases, histone demethylases and 5-methylcytosine hydroxylases, resulting in altered HIF activity, widespread chromatin alterations and a stem-like cell differentiation block (Figueroa et al., 2010; Koivunen et al., 2012; Losman et al., 2013; Lu et al., 2012; Saha et al., 2014; Chowdhury et al., 2011; Xu et al., 2011). A characteristic feature of *IDH1* mutant cancers is the CpG island methylator phenotype (CIMP or G-CIMP) (Figueroa et al., 2010; Noushmehr et al., 2010; Sasaki et al., 2012), and in experimental models, introduction of mutant *IDH1/2* and overproduction of 2-HG results in the subsequent development of global DNA hypermethylation (Figueroa et al., 2010; Sasaki et al., 2012; Turcan et al., 2012). Thus, inhibitors that decrease 2-HG levels are being investigated as potential therapeutics for *IDH1* mutant cancers (Popovici-Muller et al., 2012; Rohle et al., 2013).

In addition to these 2-HG-mediated effects, mutant *IDH1* alters canonical metabolic pathways (Reitman et al., 2014; Reitman et al., 2011; Zhao et al., 2009; Izquierdo-Garcia et al., 2014; Leonardi et al., 2012), including glutamine catabolism (Metallo et al., 2012; Seltzer et al., 2010) and the TCA cycle (Grassian et al., 2014). We therefore hypothesized that disruption of mutant IDH1 enzymatic activity would reveal metabolic dependencies that could be selectively targeted for therapeutic gain. Herein, we compared the metabolic profiles of *IDH1* mutant glioma tumor initiating cell (TIC) tumorsphere lines with and without IDH1 inhibition to identify candidate metabolic vulnerabilities.

## RESULTS

### Inhibition of Mutant IDH1 in Endogenous *IDH1* Mutant Cancer Cells Decreased 2-HG But Did Not Inhibit Cell Growth or Tumor Propagation

We recently developed *in vitro* and *in vivo* patient-derived tumor initiating cell (TIC) models of *IDH1* mutant glioma that faithfully recapitulate the histological phenotypes and genetic complexity of primary *IDH1* mutant glioma tumors (Figures S1A, S1B) (Wakimoto et al., 2014). To assess the effect of 2-HG reduction on these *IDH1* mutant TICs, we exposed cells to a well-characterized R132H and R132C IDH1 mutant specific inhibitor (IDH1i) (See Supplementary Methods and Figure S1C for details of compound chemical synthesis, structure and characterization) (Deng et al., 2015; Popovici-Muller et al., 2012). We confirmed potent inhibition of 2-HG formation *in vitro* in $IDH1^{R132H}$ mutant glioma TICs and an $IDH1^{R132C}$ mutant fibrosarcoma line (HT1080) (Figure 1A). Notably, despite 2-HG reduction, IDH1i did not inhibit *in vitro* growth of 8 endogenous *IDH1* mutant cell lines tested, including 6 glioma TICs with $IDH1^{R132H}$, HT1080 ($IDH1^{R132C}$) and an $IDH1^{R132C}$ mutant melanoma (30T) (Figure 1B). We instead observed small but consistent increases in cell proliferation in most lines (Figure 1B, Figure S1A). Our *in vitro* findings are similar to prior studies in *IDH2* leukemia models (Chen et al., 2013; Wang et al., 2013b),

chondrosarcomas (Suijker et al., 2015) and colony forming assays of *IDH1* mutant glioma lines (Turcan et al., 2013) where slight *in vitro* proliferation increases were observed with chemical inhibition of mutant IDH.

We then tested the *in vivo* effect of 2-HG depletion in an orthotopic glioma xenograft model that was derived from an *IDH1* mutant recurrent glioblastoma (MGG152) (Wakimoto et al., 2014). Treatment of mice bearing orthothopic MGG152 tumors with IDH1i (400 mg/kg twice a day) for 5 days resulted in IDHi accumulation and near-complete elimination of 2-HG within the brain tumors (Figure 1C). However, continuous daily IDH1i treatment of MGG152 orthotopic tumor bearing mice did not affect the survival of mice compared to vehicle treatment (Figure 1D). At necropsy, we observed no difference between IDH1i- and vehicle-treated animals in the size of orthotopic tumors or expression of mutant IDH1, Ki-67, GFAP or nestin within the tumors. Furthermore, no difference in *MGMT* promoter DNA methylation or H3K9 di- or tri-methylation was observed in tumor tissue (Figures S1D, S1E, S1F).

We investigated whether epigenetic alterations in endogenous mutant *IDH1* glioma cells could be reversed *in vitro* by depletion of 2-HG. Because many cycles of cell division are required to alter the epigenome after introduction of mutant *IDH1* (Turcan et al., 2012), we cultured two glioma TICs in IDH1i at concentrations sufficient to abrogate 2-HG production for up to 12 months. After 12-months, cells retained both the wild-type and mutant *IDH1* alleles and expression of the $IDH1^{R132H}$ mutant enzyme (Figures S1G, S1H). Prolonged IDH1i exposure did not detectably alter the global trimethylation or dimethylation of histone 3 lysine 9 (H3K9), global trimethylation of H3K27, genomewide distribution of DNA methylation, or the methylation of O-6-methylguanine-DNA methyltransferase (*MGMT*) gene promoter (Figure 1E, 1F, 1G). Again, we observed a persistent acceleration of cell proliferation with long-term IDH1i incubation (Figure 1H). In addition, long-term 2-HG depletion did not delay the time-to-tumor-formation or frequency of tumor initiation after implantation of *IDH1* mutant glioma TICs into mouse brains (Figure 1I). Surprisingly, long-term exposure of MGG152 to IDH1i prior to intracerebral implantation resulted in significantly shorter animal survival (Figures 1I, S1I).

We then investigated whether DNA demethylation alone or in combination with IDH1i could impact growth of *IDH1* mutant cells. We found that decitabine, but not azacytidine, decreased cell viability of MGG152 (Figure S1J). However, there was no additive or synergistic effect on cell viability with the combination of IDH1i and either decitabine or azacytidine (Figure S1K). Taken together, these data demonstrate that in some cell contexts, 2-HG levels can be uncoupled from *IDH1* mutant cancer cell proliferation, and that the cancer cell transformation induced in these endogenous *IDH1* mutant cancers is not easily reversed by depletion of 2-HG, even after many cell divisions.

## Metabolic Profiling of Endogenous *IDH1* Mutant Cancer Cells After IDH1 Inhibition Reveals a Susceptibility to Depletion of the Canonical Metabolite NAD+

Cells harboring mutant *IDH1* have altered levels of metabolites in addition to 2-HG (Grassian et al., 2014; Metallo et al., 2012; Reitman et al., 2014; Reitman et al., 2011; Seltzer et al., 2010; Zhao et al., 2009). To identify candidate metabolic therapeutic targets

other than 2-HG, we performed unbiased metabolite profiling using liquid chromatography–mass spectrometry (LC-MS) in MGG152 after short-term and long-term IDH1i incubation *in vitro* (Figure 2A, Table S1). As expected, we observed significant 2-HG reduction with both short-term and long-term IDH1i incubation. We targeted as therapeutic candidates those metabolites altered in consistent patterns in both short-term and long-term IDH1i-exposed cultures, reasoning that stable metabolic alterations may require multiple cell divisions. Other than 2-HG, only 3 metabolites were increased or reduced by 50% or greater in both short- and long-term IDH1i exposure: NADH, citrate, and glycerol-3-phosphate (G3P) (Figure 2A, Table S1).

Because G3P is a component of the NAD+/NADH shuttle system and NAD+ depletion has been investigated as a therapeutic strategy in cancer (Galli et al., 2013), we further focused on NAD+ and NADH. Using an independent method, we confirmed that IDH1i increased NADH levels in MGG152 (Figure 2B). We then discovered that IDH1i increased NAD+ in MGG152 as well as in other *IDH1* mutant lines (Figure 2C). We did not detect a significant change in NADP+ and we observed a decrease in NADPH, the substrate of the mutant IDH1/2 enzyme, after long-term IDH1i incubation (Figure 2D).

We then investigated NAD+ as a potential therapeutic metabolic target in *IDH* mutant cancer cells. We exposed cells to two chemically dissimilar, highly specific inhibitors of nicotinamide phosphoribosyltransferase (NAMPT), the rate-limiting enzyme of the NAD+ salvage pathway; FK866 (Wosikowski et al., 2002; Hasmann and Schemainda, 2003) and GMX1778 (Hjarnaa et al., 1999; Watson et al., 2009). Both NAMPT inhibitors potently inhibited cell viability of 6 endogenous *IDH1/2* mutant cancer cell lines, including 3 $IDH1^{R132H}$ mutant GBM TICs (MGG119, MGG152 and BT142), the $IDH1^{R132C}$ mutant lines HT1080 and 30T, and SW1353 chondrosarcoma ($IDH2^{R172S}$) (Figure 3A), with $IC_{50}$ values ranging between 1–25 nM (Figures 3A). In contrast, 8 *IDH1/2* wild-type cancer lines derived from similar tissue types and normal human astrocytes (NHA) were resistant at doses up to 10 μM (Figures 3A), indicative of a wide therapeutic index.

NAMPT inhibition also resulted in significant reduction of intracellular NAD+ and NADH in the *IDH1* mutant cancer cells (Figure 3B). NAMPT inhibition also decreased the production of intracellular 2-HG in *IDH1* mutant cancer cells (Figure 3C). We next tested whether the effects of NAMPT inhibitors were specifically due to reduction of NAD+ levels and on-target inhibition of NAMPT. We co-incubated *IDH1* mutant cancer cells with FK866 or GMX1778 and increasing doses of NAD+ or nicotinoamide mononucleotide (NMN), a precursor of NAD+, which bypasses NAMPT. Both NAD+ and NMN rescued *IDH1* mutant cells from the effects of FK866 and GMX1778 (Figures 3D, 3E). In addition, exogenous NMN reversed intracellular NAD+ levels, which was depleted by NAMPT inhibitor (Figure 3F). In contrast, supplementation with nicotinic acid (NA), a precursor for an alternate NAD + salvage pathway rate-limited by nicotinic acid phosphoribosyltransferase (Naprt1) (Cerna et al., 2012; Chiarugi et al., 2012; Watson et al., 2009), could not rescue *IDH1* mutant cells from the effects of NAMPT inhibition (Figure 3G).

### Mutant *IDH1* Reduces NAD+ Levels and Sensitizes to NAD+ Depletion

We measured basal intracellular NAD+ levels in our cell panel and found NAD+ to be lower in *IDH1* mutant compared to *IDH1/2* wild-type cells (Figure 4A). The relative decrease of NAD+ levels after treatment with NAMPT inhibitor was not significantly different between *IDH1* mutant and *IDH1/2* wild-type cells (Figure 4B), suggesting that the lower steady-state NAD+ pool may render *IDH1* mutant cells less able to compensate for NAMPT inhibition. We therefore hypothesized that *IDH1* mutant cells alter the dynamic steady-state supply of NAD+.

NAMPT and Naprt1 are the rate-limiting enzymes of distinct NAD+ salvage pathways that replenish the intracellular NAD+ pool. We found that expression of NAMPT did not correlate with sensitivity to NAD+ depletion, however all *IDH1* mutant cell lines examined had low or undetectable Naprt1 expression (Figure 4C). We therefore asked whether mutant *IDH1* was sufficient to alter Naprt1 expression, lower NAD+ levels, and sensitize to NAD+ depletion. We engineered MGG18, an *IDH1/2* wild-type, NAMPT inhibitor-resistant glioma TIC (Figure 3A), with a tetracycline-inducible $IDH1^{R132H}$ mutant transgene (MGG18-IDH1-R132H) (Figures 4D, S2A). Induction of $IDH1^{R132H}$ expression resulted in marked elevation of 2-HG levels (Figure S2B) as well as significantly decreased Naprt1 expression (Figures 4E), reduced intracellular NAD+ level (Figure 4F), and remarkably, induced sensitivity to NAD+ depletion (Figure 4G, S2C). We confirmed that mutant *IDH1* reduces Naprt1 expression in an isogenic system where heterozygous *IDH1* mutation has been engineered in HCT116 cells (Figure S2D). We then tested whether over-expressing Naprt1 could rescue *IDH1* mutant cells from the deleterious effects of NAD+ depletion. Lentivirus constructs carrying either *NAPRT1* driven by a constitutively active promoter (MGG152-Naprt1) or control vector (MGG152-Control) were used to infect MGG152. After stable lentiviral integration (Figure 4H), the relative NAD+ level decrease with NAMPT inhibition was mild in MGG152-Naprt1 cells but marked in MGG152-control cells (Figure 4I). In addition, this enforced NAD+ increase rescued MGG152-Naprt1 from the anti-proliferative effects of NAMPT inhibition (Figure 4J). Together, these data suggest mutant *IDH1* regulation of Naprt1 critically impacts the intracellular NAD+ pool and alters vulnerability to NAMPT inhibitors.

In cancer cells, low Naprt1 expression may be mediated by *NAPRT1* promoter methylation (Shames et al., 2013). In keeping with these prior findings, we found that the *NAPRT1* promoter CpG island was hypermethylated in our cell lines with very low Naprt1 expression, including all *IDH1* mutant lines (Figure 4K). Importantly, not all lines with low Naprt1 expression were sensitive to NAMPT inhibitors, indicating that other genetic and epigenetic factors may mediate sensitivity. As such, we observed NAMPT inhibitor efficacy in several *IDH1/2* wild-type cell lines (Figure S2E), consistent with prior reports of NAMPT inhibitor cytotoxicity in *IDH1/2* wild-type cancer cell lines (Chiarugi et al., 2012; Galli et al., 2013; Watson et al., 2009).

To assess whether alterations in observed NAD+ levels were due to changes in redox status and utilization of reducing equivalents in *IDH1* mutant cells, we calculated NAD+/NADH and NADP+/NADPH ratios after long-term IDH1i treatment, NAMPT inhibitor treatment

and mutant *IDH1* induction. These various conditions did not significantly or consistently alter NAD+/NADH and NADP+/NADPH ratios (Figures S2F-S2J). These results indicate that the effects observed with mutant *IDH1* and NAMPT inhibitors were unlikely to be mediated by changes in net redox status.

## NAD+ Depletion Disrupts TCA Cycle Metabolism in *IDH1* Mutant Cancer Cells

Because oncogenic *IDH1* mutations increase flux through the oxidative TCA cycle (Grassian et al., 2014; Cuyas et al., 2015), we investigated the effect of NAMPT inhibitors on three NAD+-requiring TCA cycle enzymes (alpha-ketoglutarate dehydrogenase, malate dehydrogenase, and isocitrate dehydrogenase) in *IDH1* mutant cells. Using LC-MS, we found that short term incubation of MGG152 with FK866 resulted in significant accumulation of TCA cycle precursors upstream of the NAD+-requiring enzymes, including citric acid, fumarate and malic acid (Figure 5). In addition, the products of NAD+-requiring enzymes in the TCA cycle, succinate and oxaloacetate, were significantly decreased. These data indicate that NAD+ depletion may compromise the TCA cycle, upon which *IDH1* mutant cells have increased dependence.

## NAD+ Depletion Induces the Intracellular Energy and Nutrient Sensor AMPK and Initiates Autophagy

Since the cell viability assay we used (CellTiter-Glo) quantitates intracellular ATP as a surrogate for cell number, we confirmed that the effects on cell viability represented cell death by counting the number of viable cells that excluded trypan blue. We found that time dependent reduction of cell number with NAMPT inhibitor exposure correlated with ATP-based cell viability assessment (Figure 6A). Cytotoxicity was not primarily mediated by apoptosis, as Annexin V, double staining for Annexin V and propidium iodide (PI), and activated caspases-3/7 did not significantly increase (Figures S3A, S3B). However, LC3-phosphatidylethanolamine conjugate (LC3-II) increased with NAMPT inhibitor exposure (Figure 6B), consistent with initiation of the metabolic-sensing pathway of autophagy, and indeed, the effects of NAD+ depletion on cell viability were rescued with the autophagy inhibitor 3-methyladenine (3-MA, Figure 6C).

We determined that autophagy was initiated by AMP activated protein kinase (AMPK), a key regulator of the metabolic checkpoint which is activated in response to nutrient- and energy-poor conditions (Hardie et al., 2007). Depletion of NAD+ in MGG152 was associated with significant phosphorylation and activation of AMPK (Figure 6D). Concomitantly, we observed activating phosphorylation of the autophagy initiating complex component ULK1 ($Ser^{555}$), which is catalyzed by AMPK (Egan et al., 2011), and activation of Atg13, another component of the autophagy initiating complex. Additionally, we observed AMPK-mediated phosphorylation of raptor and potent suppression of mTOR signaling, as illustrated by dephosphorylation of S6 ribosomal protein (S6) and eukaryotic initiation factor 4E binding protein 1 (4E-BP1). The autophagy-inhibiting activity of mTOR was therefore decreased, as noted by dephosphorylation of ULK1 $Ser^{757}$, an mTORC1 substrate (Kim et al., 2011). These findings were partially reversed by NMN supplementation, indicating autophagy initiation was an on-target effect of NAMPT

inhibition. Together, these data implicate AMPK activation as an important metabolic state sensor driving the induction of autophagy upon NAD+ depletion.

### NAD+ Depletion Inhibits *IDH1* Mutant Tumor Growth *in vivo*

To assess the *in vivo* effect of NAD+ depletion in endogenous *IDH1* mutant xenografts, we implanted HT1080 cells into the flank of SCID mice and treated with either FK866 or vehicle intraperitoneally when xenograft tumor diameters reached 5 mm. After 17 days of treatment, xenograft growth of FK866-treated animals remained near-completely inhibited while xenografts of vehicle-treated animals grew significantly (median tumor volume increase 3.2% ± 36.0% vs 415.6% ± 101.9% p=.003) (Figure 7A). There were significantly less Ki-67 positive cells in FK866-treated versus control tumors (Figure 7B).

We further tested the effect of NAMPT inhibitors on mice harboring intracerebral MGG152 glioma xenografts. One week after intracerebral implantation, animals began weekly oral dosing of either GMX1778 or vehicle. GMX1778 treatment resulted in a marked extension of survival among MGG152-bearing animals (p=.0005, log rank test) (Figure 7C). We also quantified NAD+ levels in MGG152 orthotopic gliomas 24 hours after a single dose of GMX1778, and observed near-complete elimination of intratumoral NAD+ (Figure 7D). All mice maintained good general health status and stable body weight during treatment (Figures S4A, S4B).

## DISCUSSION

Genetic evidence indicates that mutant *IDH1* is a driver of tumorigenesis and a rational therapeutic target. Targeted inhibitors of mutant IDH have shown promise in *IDH*-mutant acute leukemia patients (Cancer Discovery, 2015). However, we found that 2-HG depletion using a direct mutant IDH1 inhibitor was not sufficient to inhibit the growth of several *IDH1* mutant solid cancer types. Other genetic and/or epigenetic factors may modulate the effect of direct mutant IDH1 inhibition, and activity may be observed in only a subset of *IDH1*-mutant patients. We therefore used the direct mutant IDH1 inhibitor in an unbiased screen to identify other metabolic vulnerabilities and discovered an unanticipated and marked susceptibility of *IDH1* mutant cancers to depletion of the coenzyme NAD+, which is a critical component of intracellular signaling pathways implicated in cancer cell growth (Chiarugi et al., 2012). Depletion of NAD+ through the use of small molecule inhibitors targeting the salvage NAD+ synthesis enzyme NAMPT resulted in strikingly selective cytotoxicity in *IDH* mutant cancer cells.

Our findings indicate that mutant *IDH1* promotes this selective vulnerability by altering NAD+ supply. Introduction of mutant *IDH1* reduces expression of Naprt1, a rate-limiting enzyme within the NAD+ salvage system, and results in lower basal NAD+ levels. Exposure to NAMPT inhibitors thus effectively inhibits both NAD+ salvage pathways (NAMPT and Naprt1) in *IDH1* mutant cells, resulting in a metabolic crisis that activates the energy sensor AMPK and initiation of autophagy. In contrast, *IDH* wild-type cells have either increased expression of Naprt1 to maintain an essential supply of NAD+, or access to alternative metabolic pathways during metabolic stress (Wise et al., 2011; Mullen et al., 2012; Le et al., 2012), neither of which appear functionally-available in *IDH* mutant cancers (Leonardi et

al., 2012; Grassian et al., 2014). It is also possible that upregulated NAD+-utilizing/consuming pathways partially account for the vulnerability of *IDH1* mutant cells to NAD+ depletion. Indeed, others have demonstrated that *IDH1* mutant cells have a greater dependence on the NAD+-requiring TCA cycle (Grassian et al., 2014; Cuyas et al., 2015). Although the effects of mutant *IDH1* on NAD+-consuming pathways warrants further investigation, we find that reduced NAD+ salvage plays a major role in the mechanism of NAMPT inhibitor hypersensitivity.

The marked accumulation of 2-HG by mutant *IDH* induces global epigenetic changes (CIMP) and blocks differentiation, mediating a tumorigenic effect (Saha et al., 2014; Wang et al., 2013b). However, we did not detect epigenetic state changes nor growth inhibition of *IDH1* mutant glioma TICs with pharmacologic reduction of 2-HG. In several other model systems, only minimal alterations in CIMP and moderate inhibition of *IDH1* mutant tumor growth have been reported despite near complete abrogation of 2-HG production (Borodovsky et al., 2013; Grassian et al., 2014; Popovici-Muller et al., 2012; Rohle et al., 2013; Turcan et al., 2013). Cellular, genetic, and organ-level context likely impacts 2-HG effect and may explain the contrasting results between our models and in AML, where direct inhibition of mutant IDH2 induces differentiation of leukemia blast cells (Wang et al., 2013b). These differences suggest that *IDH1/2* mutation may have additional contributions to tumorigenesis.

Based on the available evidence, we hypothesize that *IDH* mutations induce a fertile metabolic environment upon which subsequent oncogenic alterations arise, analogous to the selection of oncogenic *KRAS* and *BRAF* mutations in hypoglycemic conditions (Yun et al., 2009). In gliomas, *IDH1* mutation occurs at the earliest stages of tumorigenesis, yet expression of IDH1 R132H is stable in TICs after multiple passages *in vitro* and *in vivo* (Borodovsky et al., 2013; Wakimoto et al., 2014) and clinically-manifest *IDH1* mutant gliomas invariably maintain the mutant *IDH1* allele despite acquiring additional malignant driver mutations (Johnson et al., 2014; Wakimoto et al., 2014). Progressive *IDH1* mutant gliomas may therefore develop and maintain vulnerability to metabolic perturbations through this context-specific development of later mutations. Exploiting such vulnerabilities could theoretically be effective against all similarly-early mutant variants of *IDH1* or *IDH2*, and may potentially be further enhanced by combination with the cellular stress induced by traditional chemotherapeutics or targeted radiation (Cairncross et al., 2014).

In conclusion, we have discovered that *IDH1* mutation can render cancer cells “addicted” to a specific metabolite, NAD+. Importantly, our findings may have rapid translational impact as NAMPT inhibitors have entered clinical development. Our study demonstrates that the paradigm of metabolic targeting can be a highly selective and potentially effective strategy for *IDH1* mutant cancers.

## EXPERIMENTAL PROCEDURES

### Cell culture, creation of cell lines, genotyping and cell line fingerprinting

Glioblastoma TICs and xenografts were generated from patient tumors as previously described (Wakimoto et al., 2009; Wakimoto et al., 2014). $IDH1^{R132H}$ overexpressing GBM

TIC (MGG18-IDH1-R132H) was generated using pLenti3.3/TR or pLenti6.3/TO/V5 containing *IDH1*$^{R132H}$, pCMV-dr8.2-dvpr and pCMV-VSVG (ViraPower HiPerform T-Rex Gateway Expression System, Invitrogen). The Naprt1 overexpressing *IDH1* mutant GBM TIC (MGG152-Naprt1) was generated using CCSB-Broad LentiORF-NAPRT Clone (GE Dharmacon), pCMV-dr8.2-dvpr and pCMV-VSVG. Cell lines were obtained from ATCC (BT142, HT1080, U87, SW1353), Sigma-Aldrich (A431), Horizon Discovery (HCT116, MCF10A) and ScienCell (NHA). 30T and UACC257 were provided by Y.S. Chemicals were purchased from Sigma-Aldrich (FK866, GMX1778, NMN, NAD+, NA, decitabine, azacytidine, and 3-MA), or Cayman (GMX1778). For long-term IDH1i exposure, IDH1i (5 μM) or DMSO (0.1%) was added to the media 2–3 times per week.

### Western Blot analyses and Immunohistochemistry

Primary antibodies for blotting: IDH1$^{R132H}$ (Dianova), H3K9me2, H3K9me3 (Abcam), H3K4me3, H3K27me3, p-AMPK, p-Raptor, p-mTOR, p-S6, p-4E-BP1, p-ULK1 (Ser$^{555}$), p-ULK1 (Ser$^{757}$), LC3B, GAPDH and Actin (Cell Signaling); NAMPT (Bethyl Labs), Naprt1 (Sigma-Aldrich), p-Atg13 (Rockland) and Vinculin (Thermo Scientific). Primary antibodies for IHC: anti-Ki-67 (1:125, Wako), Nestin (1:400, Santa Cruz), GFAP (1:400, Sigma-Aldrich), IDH1$^{R132H}$ (1:200), H3K9me3 (1:400) and H3K9me2 (1:200).

### Measurement of cell viability, cytotoxicity, autophagy and apoptosis

Cell viability was measured using CellTiter-Glo (Promega) and cytotoxicity was determined by trypan blue exclusion assay. Apoptosis was measured by staining with propidium iodide (PI) and APC-conjugated Annexin V (eBioscience) and analysis by flow cytometry (Accuri) and BD CSampler software (BD Biosciences) and by Caspase-Glo 3/7 Assay (Promega).

### Animal Efficacy Studies

$2\times10^6$ HT1080 cells were subcutaneously implanted into the right flank of 7–10-week female SCID mice. Mice were randomized to daily intraperitoneal injections of FK866 (30 mg/kg, n=6) or normal saline (n=6) for 17 days. $1–2\times10^5$ MGG152 cells were implanted into the right striatum of SCID mice. Animals were randomly assigned for oral gavage treatment with IDH1i (400 mg/kg, 2×/day), GMX1778 (250 mg/kg, 1×/week) or vehicle (20% captisol (CyDex) and 5% dextrose in distilled water). For measurements of IDH1i in tumor tissues, animals were treated for 5 days and then sacrificed. To evaluate tumorigenicity, MGG152 was cultured in DMSO or IDH1i (5 μM) for the indicated passage number then $1\times10^5$ cells were implanted intracerebrally. All mouse experiments were approved by the Institutional Animal Care and Use Committee of Massachusetts General Hospital and were performed in accordance with institutional and national guidelines and regulations.

### Liquid Chromatography-Mass Spectroscopy Data, Measurement of NAD+/NADH, NADP+/NADPH and DNA Methylation Analyses

For detailed methods of metabolite quantification, metabolite profiling, 2-HG measurement and IDHi measurement see Supp. Exp. Procedures. Genome-wide methylation analysis was performed using the Illumina Infinium HumanMethylation450 BeadChip array. Methylation

values for each site are expressed as a β value, representing a continuous measurement from 0 (completely unmethylated) to 1 (completely methylated). Methylation-specific PCR was performed in a standard two-step approach.

### Statistical analyses

Statistical analysis was performed with JMP10 software. For parametric analyses, 2-tailed t tests were used, and for analysis of frequencies of nominal data, 2-tailed Fisher exact test was used. Correlation was assessed using the Pearson's correlation coefficient. Data were expressed as mean ± SE. Survival analysis was performed using the Kaplan-Meier method and the log-rank test was used to compare survival differences between treatment arms. $p<0.05$ was considered statistically significant.

For complete details of all experimental procedures, see Supp. Exp. Procedures.

## Supplementary Material

Refer to Web version on PubMed Central for supplementary material.

## Acknowledgments

A.C. is supported by a Richard B. Simches Scholars Award and the MGH Glioblastoma Research Fund in memory of David M. King, Kirit N. Patel, Sarah E. Rippetoe and Eric W. Schwartz. D.C is supported by a Burroughs Wellcome Fund Career Award. A.C., D.C., H.W., T.B. are supported by NIH P50CA165962-01A1 (T.B., PI). T.B. is supported by NIH K24 CA125440-06. K.T. is supported by a Society of Nuclear Medicine and Molecular Imaging Wagner-Torizuka Fellowship, the Japan Brain Foundation, and the KANAE foundation for the Promotion of Medical Science. R.G. is supported by an American Heart Association Established Investigator Award. J.-R.Y. is supported by NIH R01CA140188 and the MGH Cardiology Hassenfeld Scholar Award. D.W., O.B., G.D., B.Z. and T.H. are full-time employees of Sanofi. We thank NovaBioAssays LLC for 2-HG quantitation.

## References

Amary MF, Bacsi K, Maggiani F, Damato S, Halai D, Berisha F, Pollock R, O'Donnell P, Grigoriadis A, Diss T, et al. IDH1 and IDH2 mutations are frequent events in central chondrosarcoma and central and periosteal chondromas but not in other mesenchymal tumours. J Pathol. 2011; 224:334–343. [PubMed: 21598255]

Balss J, Meyer J, Mueller W, Korshunov A, Hartmann C, von Deimling A. Analysis of the IDH1 codon 132 mutation in brain tumors. Acta Neuropathol. 2008; 116:597–602. [PubMed: 18985363]

Borodovsky A, Salmasi V, Turcan S, Fabius AW, Baia GS, Eberhart CG, Weingart JD, Gallia GL, Baylin SB, Chan TA, Riggins GJ. 5-azacytidine reduces methylation, promotes differentiation and induces tumor regression in a patient-derived IDH1 mutant glioma xenograft. Oncotarget. 2013; 4:1737–1747. [PubMed: 24077805]

Cairncross JG, Wang M, Jenkins RB, Shaw EG, Giannini C, Brachman DG, Buckner JC, Fink KL, Souhami L, Laperriere NJ, et al. Benefit from procarbazine, lomustine, and vincristine in oligodendroglial tumors is associated with mutation of IDH. J Clin Oncol. 2014; 32:783–790. [PubMed: 24516018]

Cairns RA, Iqbal J, Lemonnier F, Kucuk C, de Leval L, Jais JP, Parrens M, Martin A, Xerri L, Brousset P, et al. IDH2 mutations are frequent in angioimmunoblastic T-cell lymphoma. Blood. 2012; 119:1901–1903. [PubMed: 22215888]

Cancer Discovery. IDH1 inhibitor shows promising early results. Cancer Discov. 2015; 5:4.

Capper D, Weissert S, Balss J, Habel A, Meyer J, Jager D, Ackermann U, Tessmer C, Korshunov A, Zentgraf H, et al. Characterization of R132H mutation-specific IDH1 antibody binding in brain tumors. Brain Pathol. 2010; 20:245–254. [PubMed: 19903171]

Cerna D, Li H, Flaherty S, Takebe N, Coleman CN, Yoo SS. Inhibition of nicotinamide phosphoribosyltransferase (NAMPT) activity by small molecule GMX1778 regulates reactive oxygen species (ROS)-mediated cytotoxicity in a p53- and nicotinic acid phosphoribosyltransferase1 (NAPRT1)-dependent manner. J Biol Chem. 2012; 287:22408–22417. [PubMed: 22570471]

Chen C, Liu Y, Lu C, Cross JR, Morris JPt, Shroff AS, Ward PS, Bradner JE, Thompson C, Lowe SW. Cancer-associated IDH2 mutants drive an acute myeloid leukemia that is susceptible to Brd4 inhibition. Genes Dev. 2013; 27:1974–1985. [PubMed: 24065765]

Chiarugi A, Dolle C, Felici R, Ziegler M. The NAD metabolome--a key determinant of cancer cell biology. Nat Rev Cancer. 2012; 12:741–752. [PubMed: 23018234]

Chowdhury R, Yeoh KK, Tian YM, Hillringhaus L, Bagg EA, Rose NR, Leung IK, Li XS, Woon EC, Yang M, et al. The oncometabolite 2-hydroxyglutarate inhibits histone lysine demethylases. EMBO Rep. 2011; 12:463–469. [PubMed: 21460794]

Cuyas E, Fernandez-Arroyo S, Corominas-Faja B, Rodriguez-Gallego E, Bosch-Barrera J, Martin-Castillo B, De Llorens R, Joven J, Menendez JA. Oncometabolic mutation IDH1 R132H confers a metformin-hypersensitive phenotype. Oncotarget. 2015; 6:12279–12296. [PubMed: 25980580]

Dang L, White DW, Gross S, Bennett BD, Bittinger MA, Driggers EM, Fantin VR, Jang HG, Jin S, Keenan MC, et al. Cancer-associated IDH1 mutations produce 2-hydroxyglutarate. Nature. 2009; 462:739–744. [PubMed: 19935646]

Deng G, Shen J, Yin M, McManus J, Mathieu M, Gee P, He T, Shi C, Bedel O, McLean LR, et al. Selective Inhibition of Mutant Isocitrate Dehydrogenase 1 (IDH1) via Disruption of a Metal Binding Network by an Allosteric Small Molecule. J Biol Chem. 2015; 290:762–774. [PubMed: 25391653]

Egan DF, Shackelford DB, Mihaylova MM, Gelino S, Kohnz RA, Mair W, Vasquez DS, Joshi A, Gwinn DM, Taylor R, et al. Phosphorylation of ULK1 (hATG1) by AMP-activated protein kinase connects energy sensing to mitophagy. Science. 2011; 331:456–461. [PubMed: 21205641]

Figueroa ME, Abdel-Wahab O, Lu C, Ward PS, Patel J, Shih A, Li Y, Bhagwat N, Vasanthakumar A, Fernandez HF, et al. Leukemic IDH1 and IDH2 mutations result in a hypermethylation phenotype, disrupt TET2 function, and impair hematopoietic differentiation. Cancer Cell. 2010; 18:553–567. [PubMed: 21130701]

Galli U, Travelli C, Massarotti A, Fakhfouri G, Rahimian R, Tron GC, Genazzani AA. Medicinal chemistry of nicotinamide phosphoribosyltransferase (NAMPT) inhibitors. J Med Chem. 2013; 56:6279–6296. [PubMed: 23679915]

Grassian AR, Parker SJ, Davidson SM, Divakaruni AS, Green CR, Zhang X, Slocum KL, Pu M, Lin F, Vickers C, et al. IDH1 Mutations Alter Citric Acid Cycle Metabolism and Increase Dependence on Oxidative Mitochondrial Metabolism. Cancer Res. 2014; 74:3317–3331. [PubMed: 24755473]

Hardie DG. AMP-activated/SNF1 protein kinases: conserved guardians of cellular energy. Nat Rev Mol Cell Biol. 2007; 8:774–785. [PubMed: 17712357]

Hartmann C, Meyer J, Balss J, Capper D, Mueller W, Christians A, Felsberg J, Wolter M, Mawrin C, Wick W, et al. Type and frequency of IDH1 and IDH2 mutations are related to astrocytic and oligodendroglial differentiation and age: a study of 1,010 diffuse gliomas. Acta Neuropathol. 2009; 118:469–474. [PubMed: 19554337]

Hasmann M, Schemainda I. FK866, a highly specific noncompetitive inhibitor of nicotinamide phosphoribosyltransferase, represents a novel mechanism for induction of tumor cell apoptosis. Cancer Res. 2003; 63:7436–7442. [PubMed: 14612543]

Hjarnaa PJ, Jonsson E, Latini S, Dhar S, Larsson R, Bramm E, Skov T, Binderup L. CHS 828, a novel pyridyl cyanoguanidine with potent antitumor activity in vitro and in vivo. Cancer Res. 1999; 59:5751–5757. [PubMed: 10582695]

Izquierdo-Garcia JL, Cai LM, Chaumeil MM, Eriksson P, Robinson AE, Pieper RO, Phillips JJ, Ronen SM. Glioma Cells with the IDH1 Mutation Modulate Metabolic Fractional Flux through Pyruvate Carboxylase. PLoS One. 2014; 9:e108289. [PubMed: 25243911]

Johnson BE, Mazor T, Hong C, Barnes M, Aihara K, McLean CY, Fouse SD, Yamamoto S, Ueda H, Tatsuno K, et al. Mutational analysis reveals the origin and therapy-driven evolution of recurrent glioma. Science. 2014; 343:189–193. [PubMed: 24336570]

Kaelin WG Jr. SDH5 mutations and familial paraganglioma: somewhere Warburg is smiling. Cancer Cell. 2009; 16:180–182. [PubMed: 19732718]

Kim J, Kundu M, Viollet B, Guan KL. AMPK and mTOR regulate autophagy through direct phosphorylation of Ulk1. Nat Cell Biol. 2011; 13:132–141. [PubMed: 21258367]

Kipp BR, Voss JS, Kerr SE, Barr Fritcher EG, Graham RP, Zhang L, Highsmith WE, Zhang J, Roberts LR, Gores GJ, Halling KC. Isocitrate dehydrogenase 1 and 2 mutations in cholangiocarcinoma. Hum Pathol. 2012; 43:1552–1558. [PubMed: 22503487]

Koivunen P, Lee S, Duncan CG, Lopez G, Lu G, Ramkissoon S, Losman JA, Joensuu P, Bergmann U, Gross S, et al. Transformation by the (R)-enantiomer of 2-hydroxyglutarate linked to EGLN activation. Nature. 2012; 483:484–488. [PubMed: 22343896]

Le A, Lane AN, Hamaker M, Bose S, Gouw A, Barbi J, Tsukamoto T, Rojas CJ, Slusher BS, Zhang H, et al. Glucose-independent glutamine metabolism via TCA cycling for proliferation and survival in B cells. Cell Metab. 2012; 15:110–121. [PubMed: 22225880]

Leonardi R, Subramanian C, Jackowski S, Rock CO. Cancer-associated isocitrate dehydrogenase mutations inactivate NADPH-dependent reductive carboxylation. J Biol Chem. 2012; 287:14615–14620. [PubMed: 22442146]

Losman JA, Looper RE, Koivunen P, Lee S, Schneider RK, McMahon C, Cowley GS, Root DE, Ebert BL, Kaelin WG Jr. (R)-2-hydroxyglutarate is sufficient to promote leukemogenesis and its effects are reversible. Science. 2013; 339:1621–1625. [PubMed: 23393090]

Lu C, Ward PS, Kapoor GS, Rohle D, Turcan S, Abdel-Wahab O, Edwards CR, Khanin R, Figueroa ME, Melnick A, et al. IDH mutation impairs histone demethylation and results in a block to cell differentiation. Nature. 2012; 483:474–478. [PubMed: 22343901]

Marcucci G, Maharry K, Wu YZ, Radmacher MD, Mrozek K, Margeson D, Holland KB, Whitman SP, Becker H, Schwind S, et al. IDH1 and IDH2 gene mutations identify novel molecular subsets within de novo cytogenetically normal acute myeloid leukemia: a Cancer and Leukemia Group B study. J Clin Oncol. 2010; 28:2348–2355. [PubMed: 20368543]

Mardis ER, Ding L, Dooling DJ, Larson DE, McLellan MD, Chen K, Koboldt DC, Fulton RS, Delehaunty KD, McGrath SD, et al. Recurring Mutations Found by Sequencing an Acute Myeloid Leukemia Genome. N Engl J Med. 2009; 361:1058–1066. [PubMed: 19657110]

Metallo CM, Gameiro PA, Bell EL, Mattaini KR, Yang J, Hiller K, Jewell CM, Johnson ZR, Irvine DJ, Guarente L, et al. Reductive glutamine metabolism by IDH1 mediates lipogenesis under hypoxia. Nature. 2012; 481:380–384. [PubMed: 22101433]

Mullen AR, Wheaton WW, Jin ES, Chen PH, Sullivan LB, Cheng T, Yang Y, Linehan WM, Chandel NS, DeBerardinis RJ. Reductive carboxylation supports growth in tumour cells with defective mitochondria. Nature. 2012; 481:385–388. [PubMed: 22101431]

Noushmehr H, Weisenberger DJ, Diefes K, Phillips HS, Pujara K, Berman BP, Pan F, Pelloski CE, Sulman EP, Bhat KP, et al. Identification of a CpG Island Methylator Phenotype that Defines a Distinct Subgroup of Glioma. Cancer Cell. 2010; 17:510–522. [PubMed: 20399149]

Parsons D, Jones S, Zhang X, Lin J, Leary R, Angenendt P, Mankoo P, Carter H, Siu I, Gallia G, et al. An integrated genomic analysis of human glioblastoma multiforme. Science. 2008; 321:1807–1812. [PubMed: 18772396]

Popovici-Muller J, Saunders JO, Salituro FG, Travins JM, Yan S, Zhao F, Gross S, Dang L, Yen KE, Yang H, et al. Discovery of the First Potent Inhibitors of Mutant IDH1 That Lower Tumor 2-HG in Vivo. ACS Med Chem Lett. 2012; 3:850–855. [PubMed: 24900389]

Reitman ZJ, Duncan CG, Poteet E, Winters A, Yan LJ, Gooden DM, Spasojevic I, Boros LG, Yang SH, Yan H. Cancer-associated Isocitrate Dehydrogenase 1 (IDH1) R132H Mutation and D-2-hydroxyglutarate Stimulate Glutamine Metabolism under Hypoxia. J Biol Chem. 2014; 289:23318–23328. [PubMed: 24986863]

Reitman ZJ, Jin G, Karoly ED, Spasojevic I, Yang J, Kinzler KW, He Y, Bigner DD, Vogelstein B, Yan H. Profiling the effects of isocitrate dehydrogenase 1 and 2 mutations on the cellular metabolome. Proc Natl Acad Sci U S A. 2011; 108:3270–3275. [PubMed: 21289278]

Rohle D, Popovici-Muller J, Palaskas N, Turcan S, Grommes C, Campos C, Tsoi J, Clark O, Oldrini B, Komisopoulou E, et al. An inhibitor of mutant IDH1 delays growth and promotes differentiation of glioma cells. Science. 2013; 340:626–630. [PubMed: 23558169]

Saha SK, Parachoniak CA, Ghanta KS, Fitamant J, Ross KN, Najem MS, Gurumurthy S, Akbay EA, Sia D, Cornella H, et al. Mutant IDH inhibits HNF-4alpha to block hepatocyte differentiation and promote biliary cancer. Nature. 2014; 513:110–114. [PubMed: 25043045]

Sasaki M, Knobbe CB, Munger JC, Lind EF, Brenner D, Brustle A, Harris IS, Holmes R, Wakeham A, Haight J, et al. IDH1(R132H) mutation increases murine haematopoietic progenitors and alters epigenetics. Nature. 2012; 488:656–659. [PubMed: 22763442]

Seltzer MJ, Bennett BD, Joshi AD, Gao P, Thomas AG, Ferraris DV, Tsukamoto T, Rojas CJ, Slusher BS, Rabinowitz JD, et al. Inhibition of glutaminase preferentially slows growth of glioma cells with mutant IDH1. Cancer Res. 2010; 70:8981–8987. [PubMed: 21045145]

Shames DS, Elkins K, Walter K, Holcomb T, Du P, Mohl D, Xiao Y, Pham T, Haverty PM, Liederer B, et al. Loss of NAPRT1 expression by tumor-specific promoter methylation provides a novel predictive biomarker for NAMPT inhibitors. Clin Cancer Res. 2013; 19:6912–6923. [PubMed: 24097869]

Suijker J, Oosting J, Koornneef A, Struys EA, Salomons GS, Schaap FG, Waaijer CJ, Wijers-Koster PM, Briaire-de Bruijn IH, Haazen L, et al. Inhibition of mutant IDH1 decreases D-2-HG levels without affecting tumorigenic properties of chondrosarcoma cell lines. Oncotarget. 2015; 6:12505–12519. [PubMed: 25895133]

Turcan S, Fabius AW, Borodovsky A, Pedraza A, Brennan C, Huse J, Viale A, Riggins GJ, Chan TA. Efficient induction of differentiation and growth inhibition in IDH1 mutant glioma cells by the DNMT Inhibitor Decitabine. Oncotarget. 2013; 4:1729–1736. [PubMed: 24077826]

Turcan S, Rohle D, Goenka A, Walsh LA, Fang F, Yilmaz E, Campos C, Fabius AW, Lu C, Ward PS, et al. IDH1 mutation is sufficient to establish the glioma hypermethylator phenotype. Nature. 2012; 483:479–483. [PubMed: 22343889]

Vogelstein B, Papadopoulos N, Velculescu VE, Zhou S, Diaz LA Jr, Kinzler KW. Cancer genome landscapes. Science. 2013; 339:1546–1558. [PubMed: 23539594]

Wakimoto H, Kesari S, Farrell C, Curry WJ, Zaupa C, Aghi M, Kuroda T, Stemmer-Rachamimov A, Shah K, Liu T, et al. Human glioblastoma-derived cancer stem cells: establishment of invasive glioma models and treatment with oncolytic herpes simplex virus vectors. Cancer Res. 2009; 69:3472–3481. [PubMed: 19351838]

Wakimoto H, Tanaka S, Curry WT, Loebel F, Zhao D, Tateishi K, Chen J, Klofas LK, Lelic N, Kim JC, et al. Targetable Signaling Pathway Mutations Are Associated with Malignant Phenotype in IDH-Mutant Gliomas. Clin Cancer Res. 2014; 20:2898–2909. [PubMed: 24714777]

Wang P, Dong Q, Zhang C, Kuan PF, Liu Y, Jeck WR, Andersen JB, Jiang W, Savich GL, Tan TX, et al. Mutations in isocitrate dehydrogenase 1 and 2 occur frequently in intrahepatic cholangiocarcinomas and share hypermethylation targets with glioblastomas. Oncogene. 2013a; 32:3091–3100. [PubMed: 22824796]

Wang F, Travins J, DeLaBarre B, Penard-Lacronique V, Schalm S, Hansen E, Straley K, Kernytsky A, Liu W, Gliser C, et al. Targeted inhibition of mutant IDH2 in leukemia cells induces cellular differentiation. Science. 2013b; 340:622–626. [PubMed: 23558173]

Ward PS, Cross JR, Lu C, Weigert O, Abel-Wahab O, Levine RL, Weinstock DM, Sharp KA, Thompson CB. Identification of additional IDH mutations associated with oncometabolite R(-)-2-hydroxyglutarate production. Oncogene. 2012; 31:2491–2498. [PubMed: 21996744]

Watanabe T, Nobusawa S, Kleihues P, Ohgaki H. IDH1 mutations are early events in the development of astrocytomas and oligodendrogliomas. Am J Pathol. 2009; 174:1149–1153. [PubMed: 19246647]

Watson M, Roulston A, Belec L, Billot X, Marcellus R, Bedard D, Bernier C, Branchaud S, Chan H, Dairi K, et al. The small molecule GMX1778 is a potent inhibitor of NAD+ biosynthesis: strategy for enhanced therapy in nicotinic acid phosphoribosyltransferase 1-deficient tumors. Mol Cell Biol. 2009; 29:5872–5888. [PubMed: 19703994]

Wise DR, Ward PS, Shay JE, Cross JR, Gruber JJ, Sachdeva UM, Platt JM, DeMatteo RG, Simon MC, Thompson CB. Hypoxia promotes isocitrate dehydrogenase-dependent carboxylation of alpha-ketoglutarate to citrate to support cell growth and viability. Proc Natl Acad Sci U S A. 2011; 108:19611–19616. [PubMed: 22106302]

Wosikowski K, Mattern K, Schemainda I, Hasmann M, Rattel B, Loser R. WK175, a novel antitumor agent, decreases the intracellular nicotinamide adenine dinucleotide concentration and induces the apoptotic cascade in human leukemia cells. Cancer Res. 2002; 62:1057–1062. [PubMed: 11861382]

Xu W, Yang H, Liu Y, Yang Y, Wang P, Kim SH, Ito S, Yang C, Xiao MT, Liu LX, et al. Oncometabolite 2-hydroxyglutarate is a competitive inhibitor of alpha-ketoglutarate-dependent dioxygenases. Cancer Cell. 2011; 19:17–30. [PubMed: 21251613]

Yan H, Parsons D, Jin G, McLendon R, Rasheed B, Yuan W, Kos I, Batinic-Haberle I, Jones S, Riggins G, et al. IDH1 and IDH2 mutations in gliomas. N Engl J Med. 2009; 360:765–773. [PubMed: 19228619]

Yun J, Rago C, Cheong I, Pagliarini R, Angenendt P, Rajagopalan H, Schmidt K, Willson JK, Markowitz S, Zhou S, et al. Glucose deprivation contributes to the development of KRAS pathway mutations in tumor cells. Science. 2009; 325:1555–1559. [PubMed: 19661383]

Zhao S, Lin Y, Xu W, Jiang W, Zha Z, Wang P, Yu W, Li Z, Gong L, Peng Y, et al. Glioma-derived mutations in IDH1 dominantly inhibit IDH1 catalytic activity and induce HIF-1alpha. Science. 2009; 324:261–265. [PubMed: 19359588]

## Significance

Recently-discovered tumorigenic mutations in canonical metabolic enzymes highlight the importance of altered metabolism in cancer pathogenesis. *IDH* mutant cancers are hallmarked by aberrant accumulation of the metabolite 2-HG, which has been found to mediate many of the pathogenic phenotypes observed in these cancers. However, we found that proliferation of *IDH1* mutant solid cancers can be decoupled from 2-HG levels in some contexts. Furthermore, by systematically investigating for other metabolic vulnerabilities, we discovered that mutant *IDH1* cancers are exquisitely susceptible to depletion of the canonical coenzyme NAD+. Thus, we identify a potential therapeutic metabolic target specifically for *IDH1* mutant cancers.

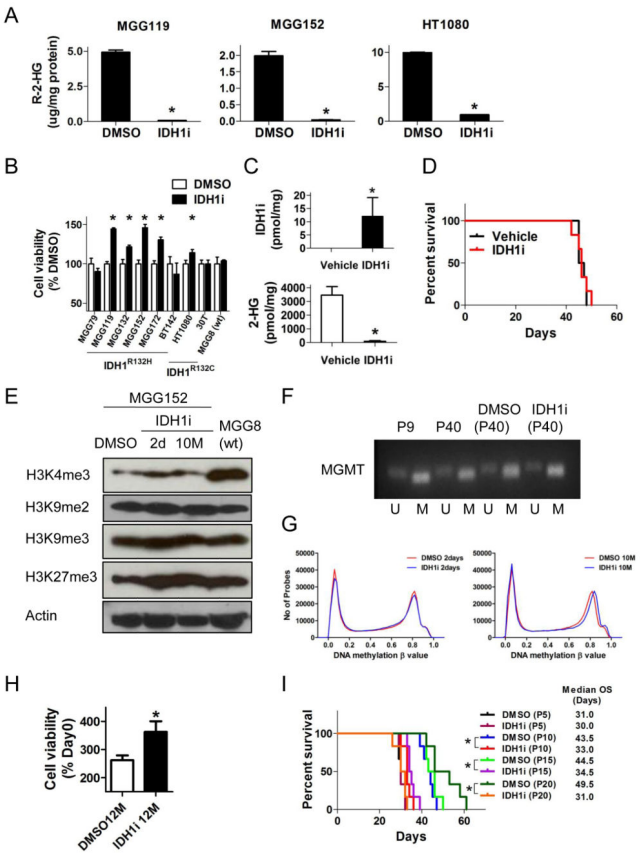


**Figure 1. Effects of mutant-specific IDH1 inhibitor in endogenous *IDH1* mutant cancer cells**

(A) R-2-HG levels in *IDH1* mutant lines (MGG119 and MGG152 have $IDH1^{R132H}$, HT1080 harbors $IDH1^{R132C}$) measured by liquid chromatography-mass spectrometry (LC-MS) +/− mutant-specific IDH1 inhibitor (IDH1i 5 μM, 48 hr) *in vitro*. (B) Cell viability assay of cell lines after incubation with IDH1i (CellTiter-Glo, normalized to DMSO control). MGG lines were analyzed at day 9, HT1080 and 30T were analyzed at day 3. (C) Concentrations of mouse MGG152 orthotopic xenograft tissue IDH1i (upper panel) and R-2-HG (lower panel) measured by LC-MS. Data were acquired after 5-day oral gavage, 2×/day, of IDH1i (400 mg/kg, n=5) or vehicle (n=5). (D) Kaplan-Meier estimates of survival by treatment. SCID mice bearing MGG152 orthotopic xenografts were randomly assigned to oral gavage of IDH1i (red, 400 mg/kg 2×/day, n=6) or vehicle (black, 2×/day, n=6). Median survival with IDH1i, 46 days (95% CI; 42–50) and with vehicle, 46 days (95% CI; 45–48, p=0.79). (E) Western blot analysis of histone methylation marks in MGG152 ($IDH1^{R132H}$) cells +/− IDH1i for 2 days or 10 months. MGG8, *IDH1/2* wild-type. Actin, loading control. (F) Methylation-specific PCR (MSP) showing *MGMT* gene promoter methylation in MGG152 +/− IDH1i. P, passage number; U, unmethylated; M, methylated. (G) Genome-wide distribution of DNA methylation in MGG152 cells treated with DMSO or IDH1i (5 μM) for 2 days ($R$=0.996, p<0.001, left) and 10 months ($R$=0.989, p<0.001, right). (H) Cell viability assay (CellTiter-Glo) of MGG152 treated with DMSO or IDH1i (5 μM) for 12 months *in vitro*. Data were obtained at day 3 and normalized to DMSO control at day 0. (I) Kaplan-Meier estimates of survival after intracerebral implantation of pre-treated MGG152. Cells

were incubated +/− IDH1i *in vitro* for the indicated cell passage number and then $1\times10^5$ cells were implanted into SCID mouse brains. Animals were then monitored for survival. In all panels: bars, +/− SEM; *, $p<0.05$. See also Figure S1.

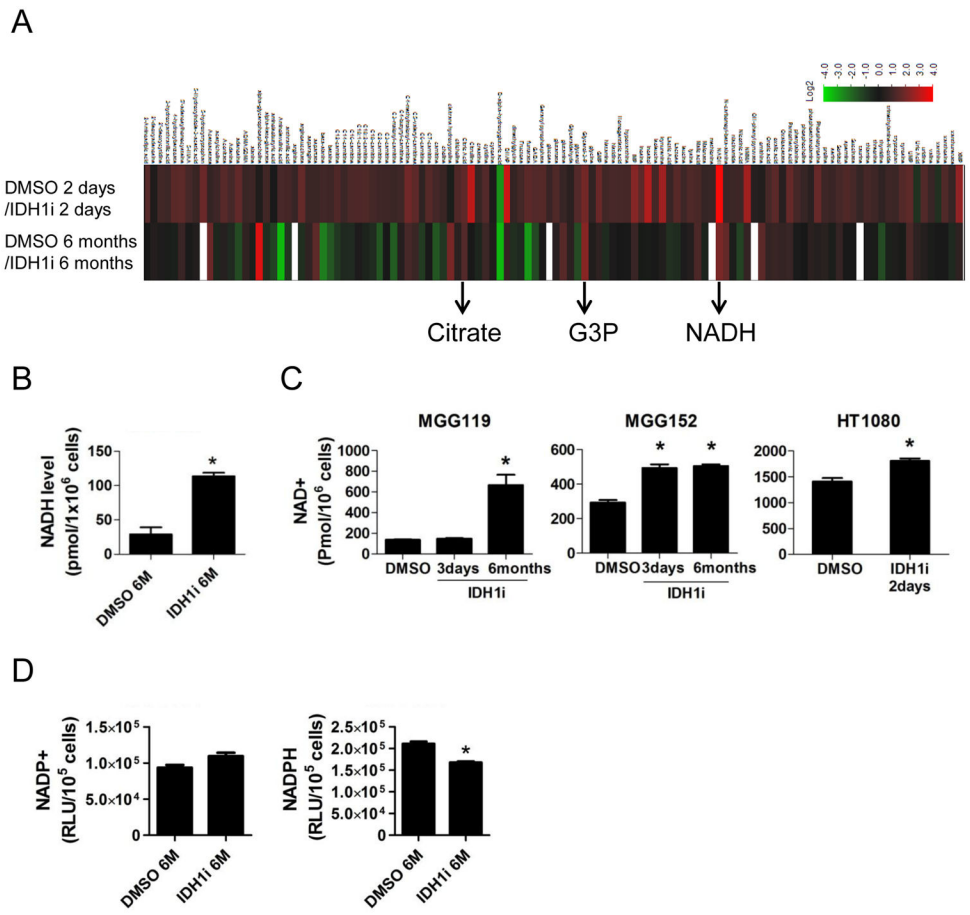


**Figure 2. Metabolic profiling after IDH1 inhibition reveals NAD+ level alterations in *IDH1* mutant cancers**

(A) Heat map representation of metabolites in MGG152 cells quantified by LC-MS. Analytes are represented as relative change with IDH1i for 2 days (upper row) or 6 months (lower row) compared to DMSO control, with increases in red and decreases in green. (B) NADH levels in MGG152 cells treated with DMSO or IDH1i for 6 months. (C) NAD+ levels in endogenous *IDH1* mutant cancer cells +/− IDH1i exposure for the indicated times. (D) NADP+ and NADPH levels in MGG152 +/− IDH1i for 6 months. Bars, +/− SEM, * $p<0.05$. See also Table S1

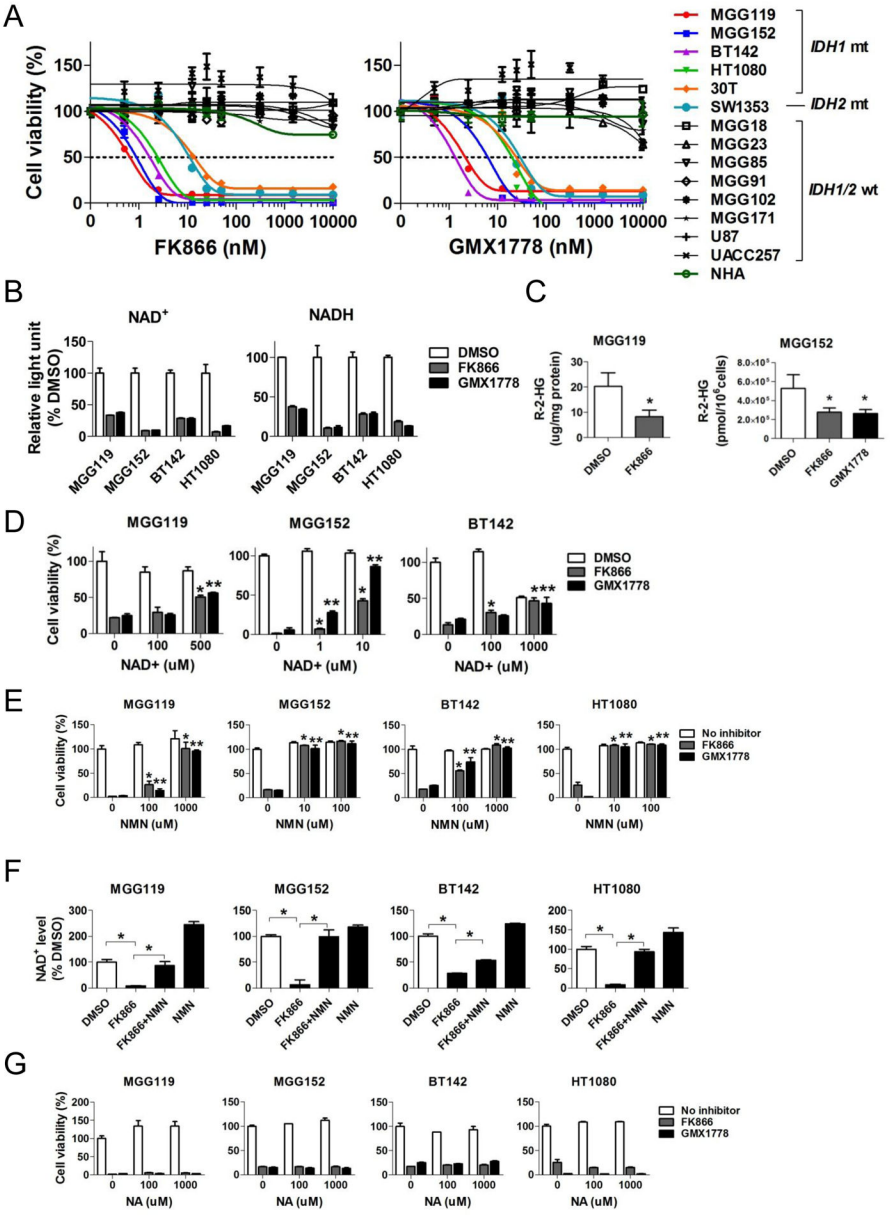


**Figure 3. NAMPT inhibitors selectively inhibit *IDH1* mutant cancers *in vitro* by depleting NAD+**

(A) Cell viability assay (CellTiter-Glo) after 72 hr treatment with FK866 (left panel) and GMX1778 (right panel). *IDH* status: $IDH1^{R132H}$: MGG119, MGG152, BT142 (gliomas); $IDH1^{R132C}$: HT1080 (fibrosarcoma), 30T (melanoma); $IDH2^{R172S}$, SW1353 (chondrosarcoma); *IDH1/2* wild-type: MGG18, MGG23, MGG85, MGG91, MGG102, MGG171, (gliomas), U87 (glioblastoma), UACC257 (melanoma) and NHA (normal human astrocytes). (B) NAMPT inhibitor effect on NAD+ and NADH levels in *IDH1* mutant cancer cells. Cells were treated with FK866 (12.5 nM, gray) or GMX1778 (12.5 nM, black) for 24 hr prior to measurement. Data are represented as %DMSO control. (C) R-2-HG levels measured by LC-MS in *IDH1* mutant cells +/− incubation with FK866 (12.5 nM, 48 hr, gray) or GMX1778 (12.5nM, 48 hr, black). (D) and (E) Cell viability assay of *IDH1* mutant

lines incubated with FK866 (12.5nM, 72 hr) or GMX1778 (12.5nM, 72 hr) and increasing concentrations of exogenous NAD+ (72 hr, D) or nicotinamide mononucleotide (NMN, 72 hr, E). *, $p<0.05$ for difference between addition of NAD+ or NMN vs. FK866 alone; **, $p<0.05$ for difference between addition of NAD+ or NMN vs. GMX1778 alone. (F) Relative NAD+ levels in *IDH1* mutant cancer cells 24 hours after treatment with FK866 (12.5 nM), NMN (1 mM), or the combination of FK866 (12.5 nM) and NMN (1 mM) vs. DMSO (24 hr) control. (G) Cell viability assay of *IDH1* mutant cancer cells incubated with FK866 (12.5 nM, 72 hr) or GMX1778 (12.5 nM, 72 hr) and increasing concentrations of exogenous nicotinic acid (NA, 72 hr). Bars, +/− SEM, * $p<0.05$.

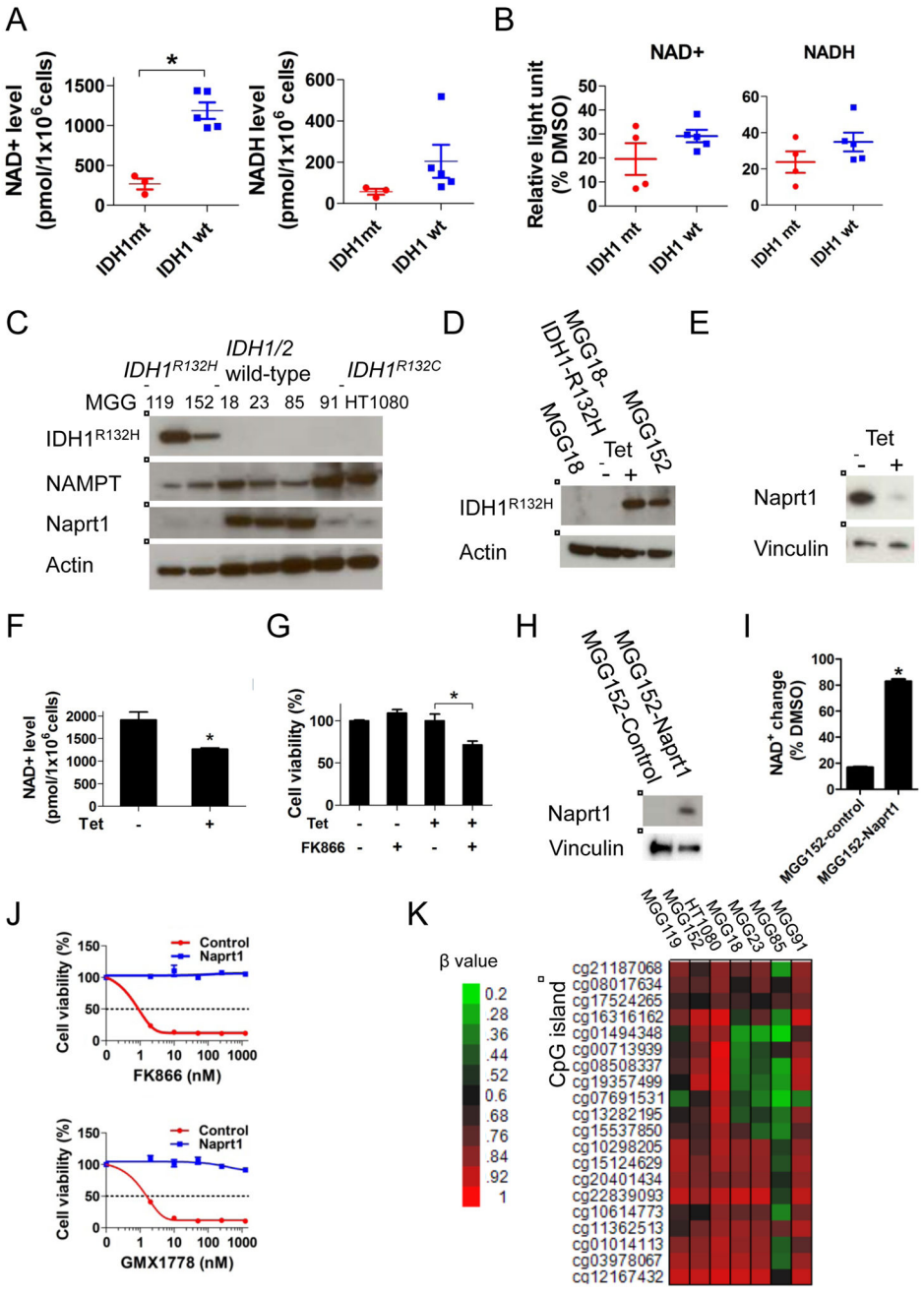


**Figure 4. *IDH1* mutation reprograms NAD+ metabolism**

(A) Scatter plots of absolute NAD+ (left panel) and NADH (right panel) levels in a panel of glioma tumorsphere lines. (B) Relative NAD+ and NADH decrease after FK866 (12.5 nM, 24 hr) treatment of the lines in panel A compared to DMSO control (24 hr). (C) Western blot analysis of $IDH1^{R132H}$, NAMPT and Naprt1. Actin, loading control. (D) and (E) Western blot analysis of MGG18 (*IDH1/2* wild-type) engineered with a tetracycline (tet)-inducible $IDH1^{R132H}$ gene (MGG18-IDH1-R132H). MGG18-IDH1-R132H was incubated +/− tet for 2 months *in vitro*, then harvested for analysis. Actin, Vinculin, loading controls. (F) NAD+ levels of MGG18-IDH1-R132H cells +/− tet induction for 2 months. (G) Cell

viability assay of MGG18-IDH1-R132H cells +/− tet induction for 2 months followed by +/− FK866 (12.5nM, 5 days). (H) Western blot analysis of MGG152 infected with lentivirus carrying no (MGG152-control) or Naprt1 cDNA (MGG152-Naprt1). Vinculin, loading control. (I) Relative NAD+ change after FK866 treatment (12.5 nM, 24 hr) in MGG152-control and MGG152-Naprt1 compared to DMSO control (24 hr). (J) Cell viability assay of MGG152-control and MGG152-Naprt1 after 48 hr incubation with FK866 or GMX1778. (K) Heatmap of *NAPRT1* promoter DNA methylation status in *IDH1* mutant (MGG119, MGG152 and HT1080) and *IDH1/2* wild-type (MGG18, MGG23, MGG85 and MGG91) lines measured by Infinium arrays. β values represent the fraction of methylated CpG site. Data were acquired by Infinium HumanMethylation 450 BeadChip array. Bars, +/− SEM, * $p<0.05$. See also Figure S2.

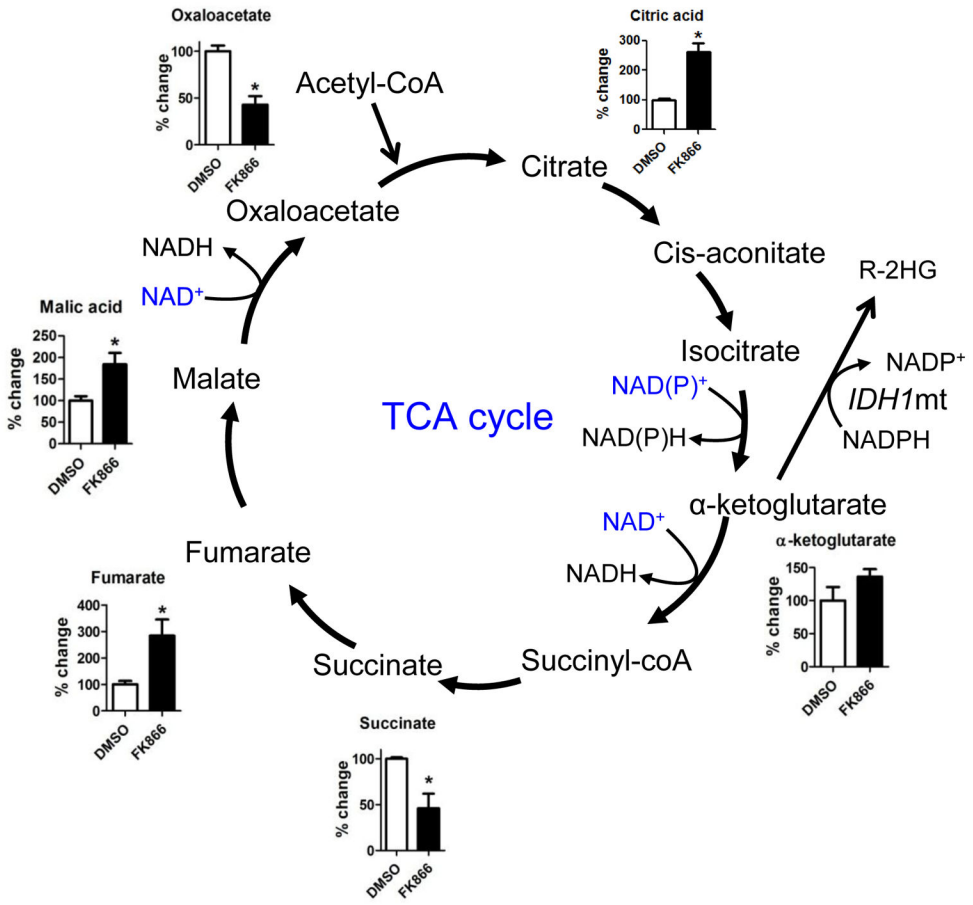


**Figure 5. NAMPT inhibitor effect on NAD+-utilizing pathways in *IDH* mutant cancers**

Metabolites of the tricarboxylic acid (TCA) cycle in MGG152 cells were quantified by LC-MS after treatment with DMSO (36 hr, white bars) or FK866 (12.5 nM, 36 hr, black bars). Bar graphs represent the changes in FK866-treated cells relative to DMSO control.

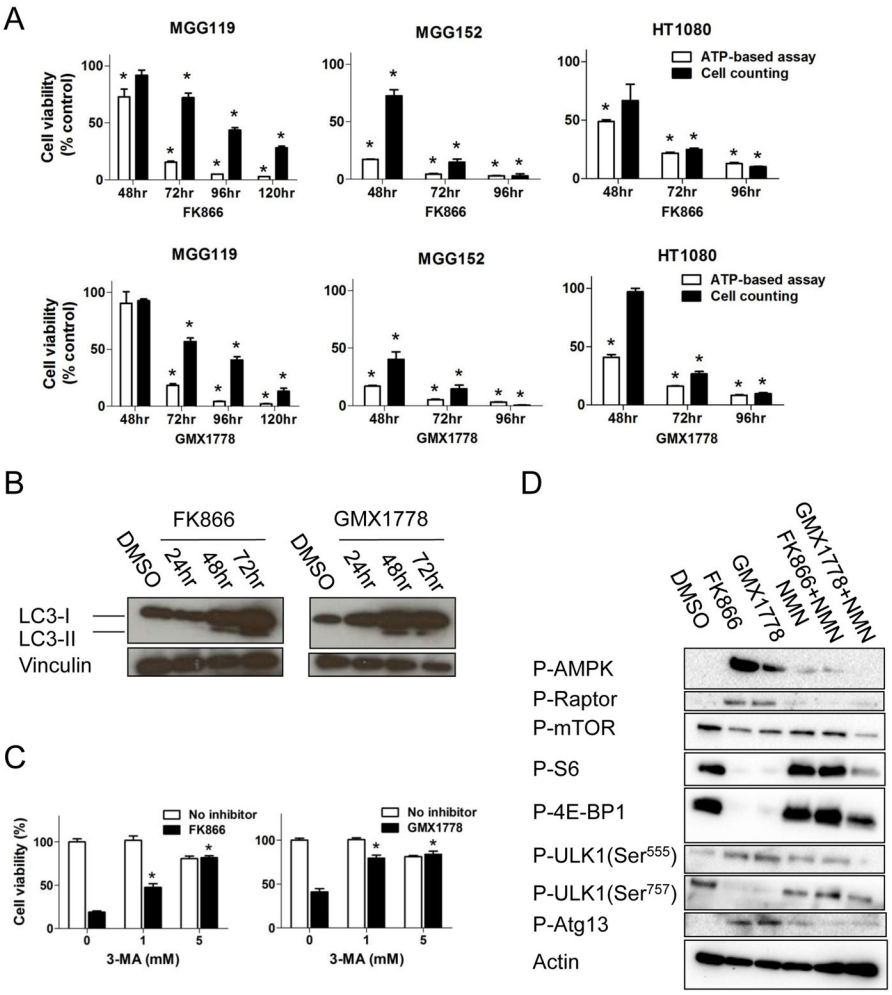


**Figure 6. NAD+ depletion triggers AMPK-initiated autophagy and cell death in *IDH1* mutant cancer cells**

(A) Relative cell viability of cells treated with FK866 (upper row) and GMX1778 (lower row) measured by CellTiter-Glo (white bars) and viable cell count (Trypan blue exclusion assay, black bars) compared to DMSO controls. (B) Western blot analysis of LC3-I and LC3-II expression in MGG152 cells after treatment with FK866 (12.5 nM) and GMX1778 (12.5 nM) compared to DMSO control (72 hr). Vinculin, loading control. (C) Cell viability assay (CellTiter-Glo) of MGG152 cells treated for 72 hr with FK866 (12.5 nM, left), GMX1778 (12.5 nM, right), or DMSO +/− autophagy inhibitor 3-methyladenine (3-MA). Bars, +/− SEM, * $p<0.05$. (D) Western blot analysis of MGG152 cells treated with DMSO (48 hr), FK866 (12.5 nM, 48 hr), GMX1778 (12.5 nM, 48 hr) and NMN (100 μM, 48 hr) alone and in combinations as indicated. Actin, loading control. See also Figure S3.

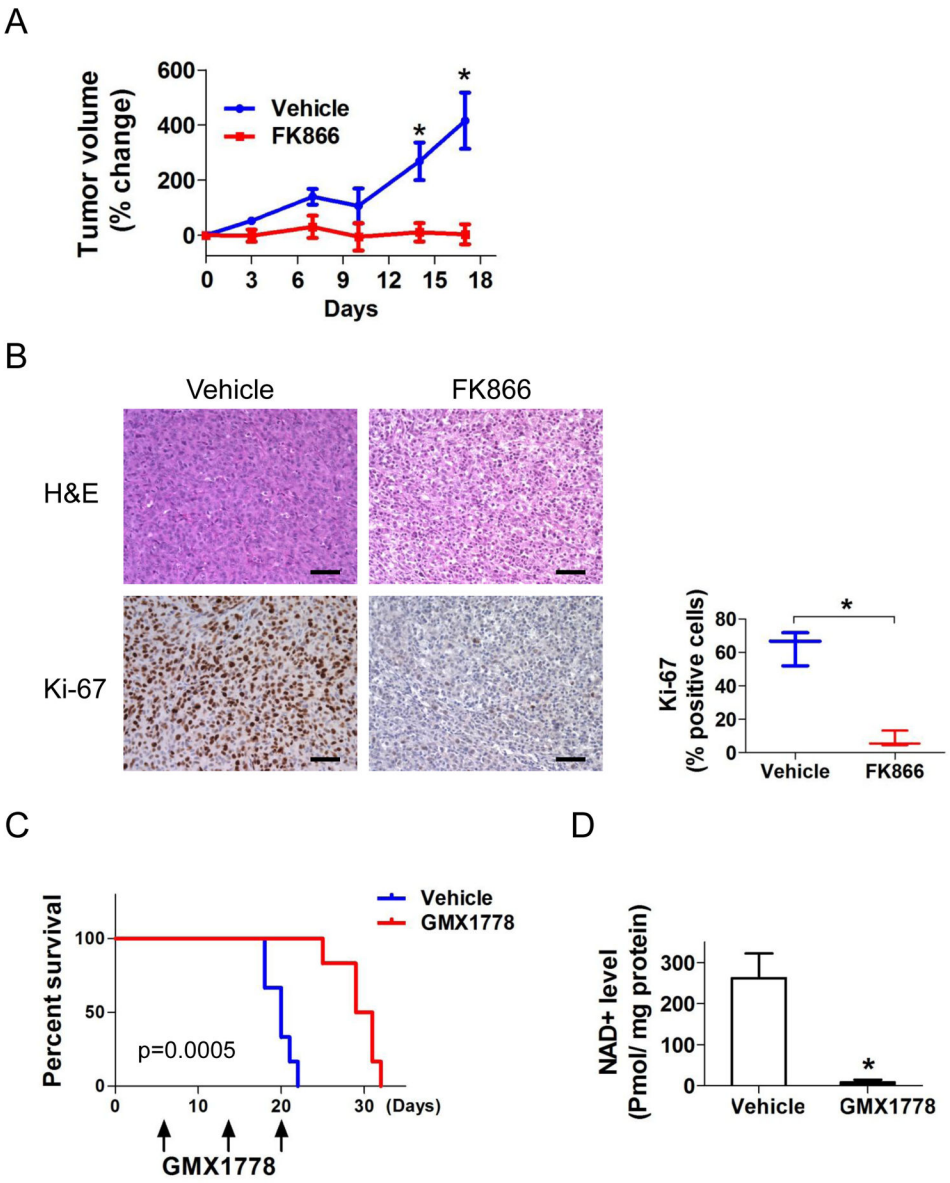


**Figure 7. NAMPT inhibitors inhibit growth of *IDH1* mutant xenograft tumors**

(A) SCID mice implanted with HT1080 (*IDH1*$^{R132C}$) cells in the flank were randomly assigned to intraperitoneal injections (4 days/week) of FK866 (30 mg/kg, n=6) or vehicle (n=6). Day 0 (treatment initiation) was the baseline. (B) Hematoxylin and eosin (H&E) and Ki-67 staining of HT1080 xenograft tissues. Ki-67 staining index: 63.5 ± 10.3 % (vehicle, left) vs 7.7 ± 4.8% (FK866, right) p=.001. Scale bars, 100μm. (C) Kaplan-Meier estimates of survival by treatment. SCID mice intracerebrally implanted with $2\times10^5$ MGG152 cells were randomly assigned to oral gavage (1/week) of either GMX1778 (250 mg/kg, n=6) or vehicle (n=6). (D) NAD+ levels in MGG152 orthotopic xenografts measured 24 hr after one dose of GMX1778 (250 mg/kg, black bar) or vehicle (white bar). Bars, +/− SEM, * p<0.05. See also Figure S4.